

THREE-DIMENSIONAL IN-PROCESS TEMPERATURE MEASUREMENT OF LASER SINTERED PART CAKES

Stefan Josupeit and Hans-Joachim Schmid

Direct Manufacturing Research Center (DMRC) and Particle Technology Group (PVT),
University of Paderborn, Germany

Contact: stefan.josupeit@dmrc.de

REVIEWED

Abstract

An uneven temperature distribution and varying cooling rates at different positions within the part cake are two of the most important challenges regarding the part quality and reproducibility of the polymer laser sintering process. In the presented work, a temperature measurement system is implemented within an EOSINT P395 laser sintering system. It allows the determination of a three dimensional temperature distribution and history during the full build and cooling process. The influence of important job parameters, for example the packing density, job height and layer thickness, can be figured out. In combination with a finite element simulation of the cooling process, the temperature measurement will be the basis for optimized process controls.

Introduction

In the polymer laser sintering process, parts are manufactured layerwise out of a powder by laser exposure. The unmolten powder surrounds and supports the built parts. After the building process finishes, the part cake including the parts cools down from the exterior to the interior areas, and thus inhomogeneous at different positions within the part cake. Job parameters like the packing density or the job height also influence the cooling rate. In addition, this effect may influence the recrystallization behavior and thus also part quality characteristics like mechanical part properties, warpage or shrinkage effects. These uncertainties regarding the cooling process are one of the most important challenges regarding the reproducibility and process quality of the whole manufacturing process. As a result, an analysis of the temperature distribution and history is essential for the development of optimized process controls, in which the varying cooling rates and their influence on part quality characteristics are considered.

In this work, a temperature measurement system is implemented within an EOSINT P395 laser sintering system from EOS Electrical Optical Systems, Krailling, Germany. The measurement system is used to determine the temperature distribution within the part cake during the whole manufacturing process from the warming up phase to the end of the cooling process. The temperature is determined using more than 50 thermocouples attached to tubes penetrating the part cake from the bottom. As a first step, the reproducibility of the measurement method is shown repeating the same experimental set-up three times. In a second step, the temperature distribution and history is analyzed.

The chapter “state of the art” describes past publications and papers related to this topic identifying the need for a cooling analysis. The development and construction of the temperature measurement system as well as the test set-up is given in the “method” chapter followed by the visualization and interpretation of the measurements in the “result” chapter. The work is concluded with a summary and an outlook towards future process investigations and optimizations.

State of the Art

Although the importance of the part cake cooling process and the position dependency of powder and part properties have been identified in various works, investigations of the inner part cake temperature distribution and history can only rarely be found in common literature. Most investigations are based on an analysis of the powder bed surface temperature. This chapter will emphasize the significance of an extensive cooling analysis and give an overview about previous approaches.

Rüsenberg et al. investigated the impact of different cooling procedures on the mechanical tensile properties of laser sintered polyamide 12 parts. It was found out that a longer cooling phase with a low unpacking temperature ($\sim 50^{\circ}\text{C}$) lead to a significantly lower elongation at break compared to specimens unpacked earlier ($\sim 140^{\circ}\text{C}$). No influence was observed regarding the tensile strength. This effect can be traced back to a lower crystallinity level using a higher cooling rate. However, the reproducibility from job to job and within one job was worse when unpacking the job earlier. As a result, the cooling process should be given a high importance within the laser sintering process chain [RWF+12][RJS14].

Wegner et al. identified an inhomogeneous temperature distribution on the powder bed surface and an inhomogeneous cooling process as main reasons for a bad reproducibility of the laser sintering process for different machine types. Temperature measurements were performed using thermal imaging for the surface and four wireless sensors in the bottom build area for the inner powder bed. The surface temperature directly influences the mechanical part properties, density and dimensional accuracy. Since the powder bed already cools down partially during the build process and inhomogeneous in general, the part properties are dependent on the position within the build volume and the part geometry itself. The powder bed temperature indicated an isothermal process. In addition, the effect of melt temperature was studied. Reducing the temperature gradients during the build and cooling process has already been proven using optimized temperature controls and is suggested for a higher reproducibility in future machine generations [WW13][WW14].

Soe et al. also considered the dimensional accuracy of laser sintered parts induced by shrinkage effects in (upright) z direction. Parts built in the corners of the build area showed a lower and less uniform shrinkage compared to parts built in the center. These observations were related to temperature gradients on the powder bed surface as well as different cooling rates during the post-build cooling phase [SES13].

Similar investigations were earlier made by Shen et al., where the three-dimensional temperature distribution within the part cake was identified as main influencing factor on the dimensional part accuracy. Since the inner part cake temperature varies from job to job due to different packing densities, a simulation of the laser sintering process is suggested to compensate shrinkage effects in the whole build volume [SSG+00]. Measurements of the inner part cake temperature were provided by Steinberger, who inserted 12 PT-100 sensors from the side walls into the part cake. Thereby, supporting structures had to be sintered to fix the sensors [Ste01].

Time and temperature dependent crystallization effects of polymer laser sintering materials in general were investigated by Rietzel et al. using regular and isothermal DSC analysis, a plate-plate rheometer and pvT measurements. The time between phase changes in isothermal experiments using polyamide 12 changes significantly, for example from 21.9 min (168°C) to 77.6 min (171°C). As a result, the temperature history of the material during the build and cooling process is essential for the crystallization behavior and thereby, due to possible curl effects, also the processability [RDK+11].

Method

The aim of the presented temperature measurement is to determine the inner temperature distribution and history of the part cake. Thereby, various requirements are considered:

- measurement during the full build and cooling process
- implementation of >50 measurement points for a wide data base spread throughout a wide and representative region within the exchangeable frame
- no or only slight manipulation of the build process and temperatures
- consideration of kinematic restrictions due to moving machine parts

As a result, the main function and sub-functions are identified and structured (figure 1).

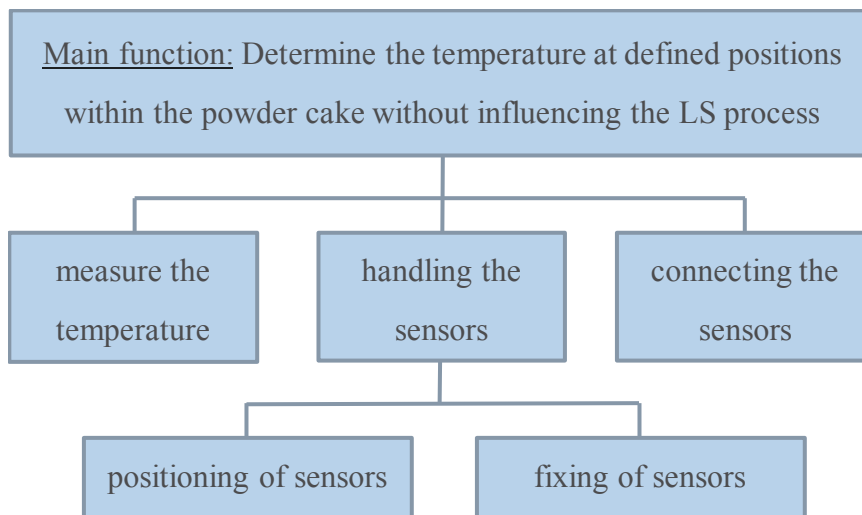


Figure 1: Structured (sub-) functions of the temperature measurement system

In total, three different measurement concepts were developed. Here, only the chosen concept illustrated in figure 2a is described. It is based on the construction of sensor bars, which are attached to brackets at the bottom of the exchangeable frame. Two narrow brackets are positioned at the left and right frame edge and fix the thermocouples in the build frame edges. One larger bracket is attached in the lower front and fixes all sensor bars in the inner build area. The lift mechanism moving the build stage is not influenced by the system, so that the full build volume can still be used. However, some modifications are required in the machine to prevent a collision between the front bracket and the mounting of the build stage. Holes are drilled into the build stage at the sensor positions. During the build job (movement of the build stage), the thermocouples slowly penetrate the part cake from the bottom. When the part cake cools down, the sensors have a fixed position relative to the frame and part cake.

The sensor bars itself consist of fiberglass reinforced plastic tubes with an outer diameter of 8 mm and a wall thickness of 1 mm. Within these tubes, up to eight fiberglass coated thermocouples (type T) are fixed using high-temperature silicone. The test prods are located at the tube surface through small drilled holes. Here, a sensor distance of 45 mm in z direction is chosen, which results in a total measurement length (= test build height) of 300mm. For other measurement lengths, also shorter or longer configurations can be produced. In addition, one thermocouple is located on the top of each tube in order to measure the temperature 3-4 mm beneath the powder bed surface. The top area of a sensor bar is pictured in figure 2c.

Regarding the positioning of the sensor bars, the right front eighth of the build area is chosen for an extensive analysis (figure 2b) with six sensor bars containing eight thermocouples each. Three further sensor bars with two thermocouples each are placed in the other three corners to validate if the chosen edge is representative for the whole part cake. In total, this means a density of 54 thermocouples within the part cake, ensuring a large data basis for the whole build area.

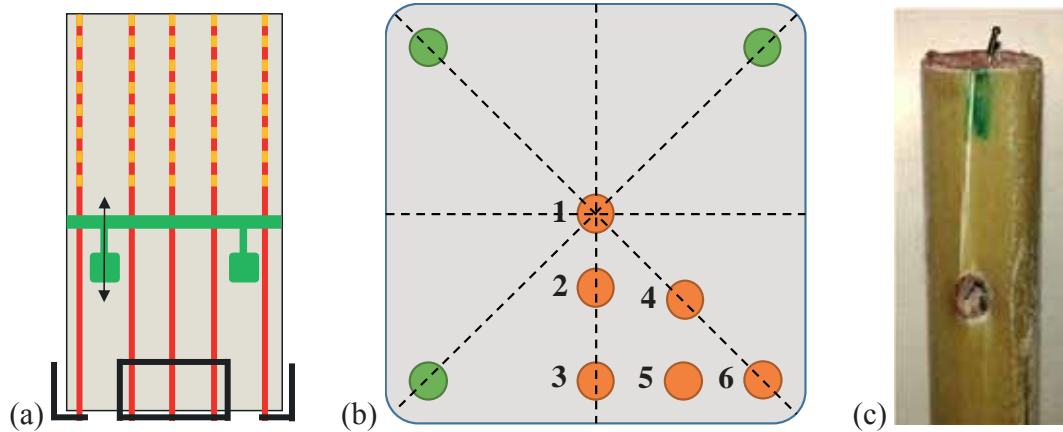


Figure 2: (a) schematic sketch, (b) sensor bar positions, (c) close-up photo of a sensor bar

The thermocouples are connected to two *Expert Key 200L* measurement devices from *Delphin Technology*, Bergisch Gladbach, Germany. Each of these devices offers 28 thermocouple channels, of which 8 can also be used with PT sensors. To reduce the measurement uncertainties, two PT-100 sensors are additionally connected to the systems. All 56 sensors are placed in a scientific furnace for a two-point calibration at 40 and 180°C using the PT-100 sensors as reference. To reduce the influence of environment changes, the measurement devices are additionally put into laser sintered boxes. After these steps, the variance of the measured temperature values is $\pm 0.5\text{K}$.

For the first part-less test jobs, the parameters given in figure 3 are used. The experimental set-up is reproduced three times and shall give information about the measurement accuracy and deviations from job to job.

build height	300 mm
powder quality	100% recycled PA 2200 powder, MVR = 12 cm ³ /10min
layer thickness	120 μm (EOS Part Property Profile “Balance”)
pre-heating phase	4 h
adjusted temperatures	process chamber: 180°C; removal chamber: 130°C
cooling phase	10 h within machine (nitrogen) + >24 h outside (standard atmosphere) until <50°C
build time	~ 14 h 45 min
build speed	~ 20.3 mm/h
part packing density	0% → no parts

Figure 3: Job parameters of the first test jobs to examine the experiment repeatability

Results & Discussion

To analyze the temperature profiles during the build and cooling process, the data frequency of the measured temperatures is first reduced from 1/5s to 1/300s for all sensors. In figure 4, the whole build process is shown for all thermocouples of the (center) sensor bar 1. Thereby, the measurement height represents the distance from the bottom (0 mm) to the top of the job (300 mm). The process can be divided into four phases: Phase I is the pre-heating phase. During this phase, the thermocouples measure the removal chamber temperature beneath the build platform. The temperature is constant after approximately 2 hours at $\sim 148^{\circ}\text{C}$. The next phase II is the build phase itself. One after another, the temperature sensors penetrate the part cake, so that the temperature rises from the removal chamber temperature to the inner part cake temperature. There is a relative movement between powder and sensor bar, which means that the temperatures shown here belong to a fixed position regarding the build frame and not the part cake. The transition between phase II and III represents the initial temperatures when the cooling process starts. Phase III and IV are the two cooling phases within the machine and in standard atmosphere. A “buckling” between these curves can only be seen for thermocouples close to the frame edges; the cooling fastens afterwards. It is also obvious that the bottom area cools down earlier and faster than the top area. The maximum temperature during cooling is between a build height of 150 and 195 mm.

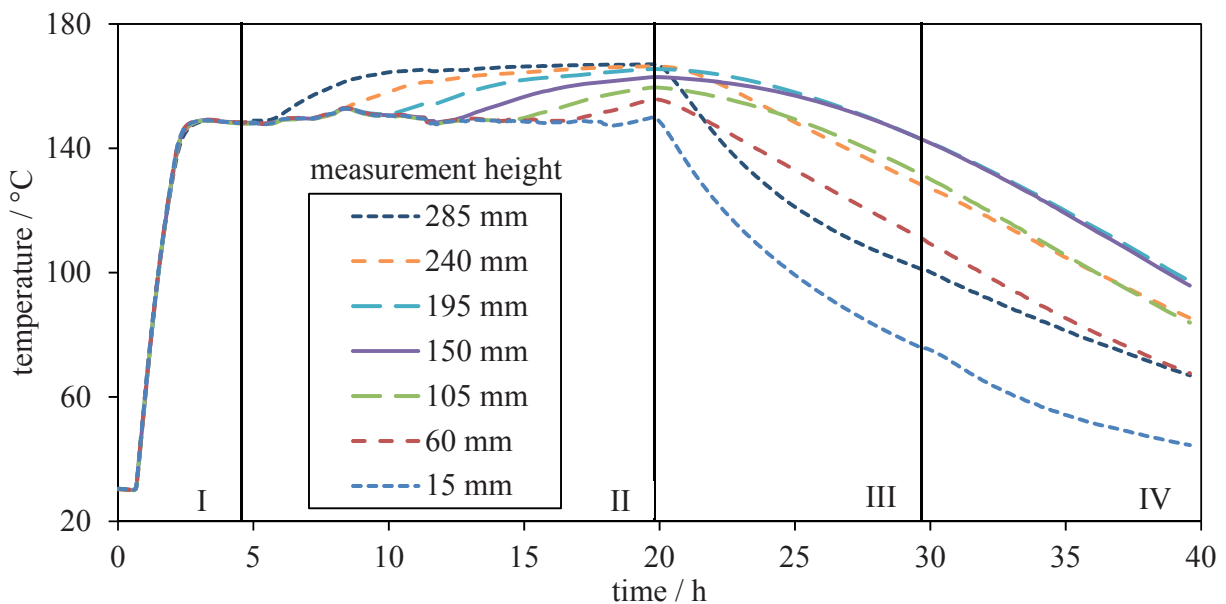


Figure 4: Temperature profile for the (center) sensor bar 1 at different z heights

Due to the relative movement of the powder and the sensors during the build process, the temperature history of fixed positions within the powder cannot be measured directly, but calculated considering the build speed. This is shown for the sensor bars 1 and 6 in figure 5. Powder recoated in a distance of 15 mm from the build stage does not change its temperature during the build process. The longer the job build, the higher and steadier is the temperature 3-4 mm beneath the top layer. As a result, the “cooling process during build” is not isothermal for higher builds and dependent on heat flux into and from the recoated powder. The profile for sensor bar position 6 is the same in shape, but lower in absolute temperatures due to the short distance to the frame edges.

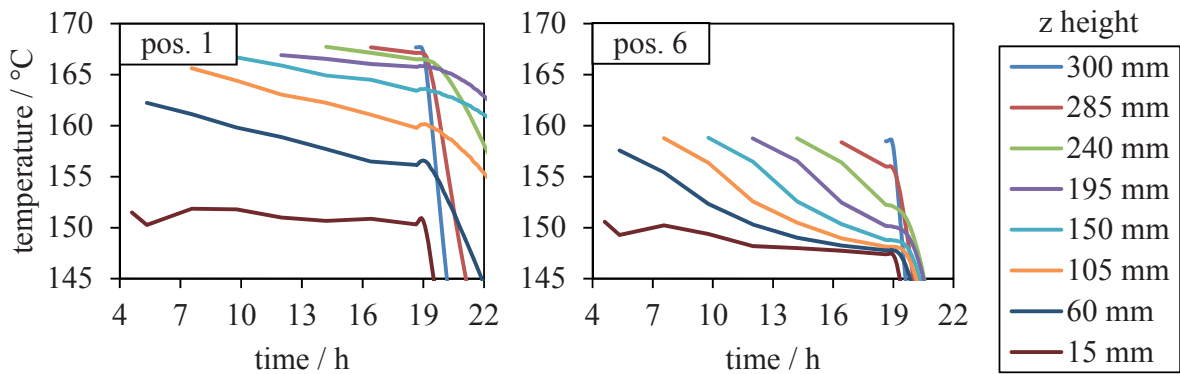


Figure 5: Calculated temperature profile for fixed positions within the part cake during build

To consider the reproducibility of the measured temperatures, the standard deviation from test job 1 to 3 is calculated for all sensors during the whole cooling process. The average standard deviation for every sensor bar is given in figure 6. It is obvious that the standard deviations in the sensor bars 2 and 3 are the highest with values about 2.7 K. This can be traced back to outliers in the center areas of these bars. A possible reason for that are cracks that occur during the cooling of the part cake. Depending on where the cracks open up exactly, the measurement may be influenced. The standard deviations of all other sensor bar positions are very close to the measurement accuracy (~1 K) and therefore negligible.

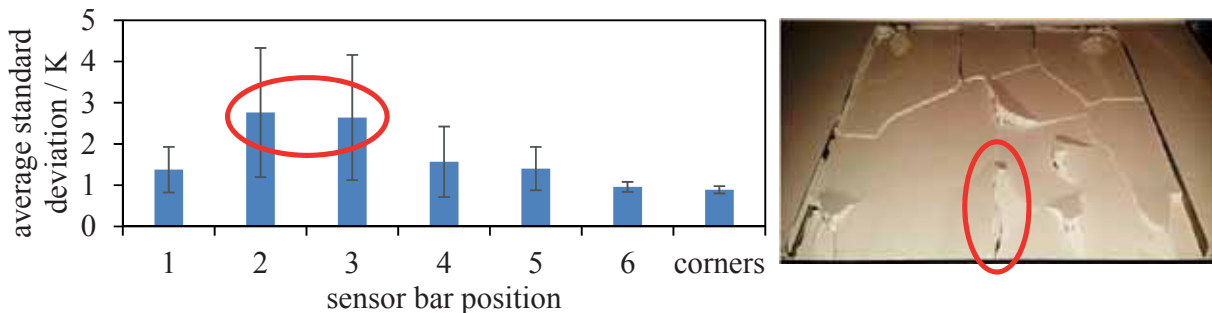


Figure 6: Average standard deviation from test job 1 to 3 during the cooling phase (left) and cracks on the part bed surface (right)

A closer view onto the temperature profile in z direction during the cooling process is given in figure 7. On the left hand side, the temperature profile for the (center) sensor bar 1 is shown. The blue graph on the right represents the initial temperature distribution at cooling start. The temperature gradient between the top and bottom placed thermocouple is about 17 K. After 4 hours of cooling within the machine it is visible that the up and down areas cool much faster than the center area of the part cake. Between a cooling time of 4 and 20 hours, the gradient is much higher compared to the initial profile and kind of parallel shifted; an influence of the change of the environment conditions at 10 hours cannot be seen directly. Approaching a maximum temperature of 50°C, the temperature gradient along the z axis decreases again. The position of the maximum temperature shifts down from the top area to a z height of approximately 175 mm during the cooling process. In contrast, the cooling within the right front corner (position 6, right graph) is much faster and more homogeneous considering the temperature gradients in z direction; however the temperature gradients in the x/y plane (not shown here) are much higher in this area.

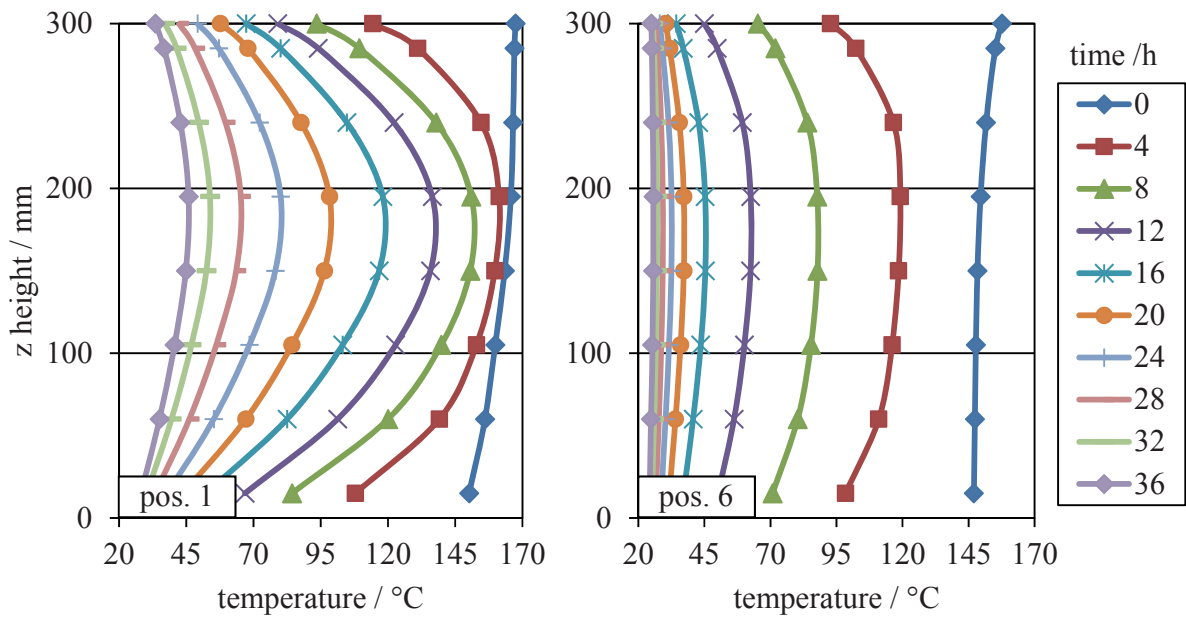


Figure 7: Time dependent temperature profile along the z axis for the sensor bar positions 1 and 6 during the cooling process starting at $t = 0$ h

The three-dimensional temperature distribution at different time steps is also visualized using *Matlab* and is shown as quarter models in figure 8. The empty voxels represent the area where no measurement was performed, which is a distance of 33 mm to the outer frame edges and 15 mm to the build stage.

The upper left image presents the initial temperature distribution when the cooling starts. Thereby, the highest temperature (167°C) is found in the upper center of the build area, while the lowest temperature is determined in the bottom corner of the build frame (147°C). After a cooling time of 3 hours (upper right image), the top and bottom areas have already cooled down to approximately 110°C . The temperature gradient in z direction here is higher in z direction than in the x/y plane. It has to be considered that the outer areas are missing in the measurement and that higher gradients are expected in this regions. Also, confirming the observations of the upper analysis, the position of the hottest point shifts down.

After 10 hours, elliptic isothermal shells around the center in a z height of about 175 mm can be observed. In this phase, the gradient between the hottest and the lowest measured temperature is about 90 K. After another 10 hours, the outer part cake regions are kind of “uniform” again. Only the temperatures in the center area change significantly afterwards.

Although the temperature measurement system delivers plausible and highly reproducible results, there are still a few challenges to be approached. Due to the fixed position of the sensor bars and the relative movement to the powder during the build phase, the powder hardens above the sensor bars because it is heated up in every layer. These “cakes” break off several times during the build process. The prevention of this effect is under investigation.

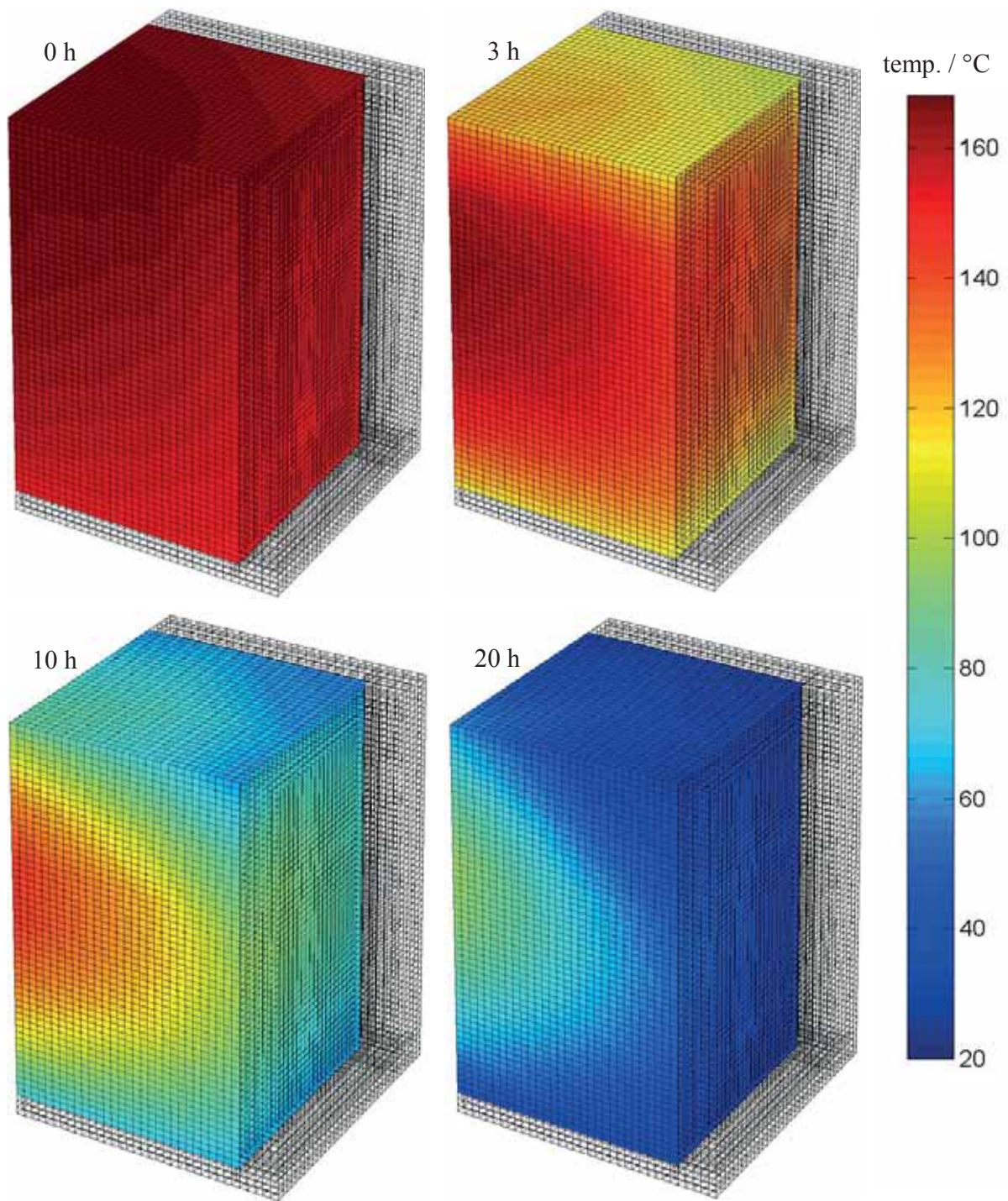


Figure 8: 3D plots of the measured temperature distribution during the cooling process

Conclusions & Outlook

In the presented work, a temperature measurement system to determine the inner powder cake temperature distribution and history has been developed. In contrast to earlier studies, the measurement is based on much more and denser data points. Also, a measurement during the whole build and cooling phase is possible. The measurement system offers a high reproducibility: most of the deviations from job to job are within the measurement accuracy. Deviations at specific positions within the part cake may be traced back to the occurrence and influence of cracks.

Several temperature profiles and gradients during the cooling process have been analyzed. The temperature profile of different positions within the powder during the build phase reveals an interaction between heat flux into (process chamber) and from (removal chamber) the powder, which results in an isothermal profile for low build heights and a decreasing profile for bigger build heights. The final cooling in the lower part cake is faster than in the upper areas due to different initial temperatures when the cooling starts. Nevertheless, the temperature gradients developing during the build phase are much lower compared to the gradients during the cooling phase.

In further studies, the effect of important job parameters on the cooling behavior will be investigated. For example, the influence of the build height will be significant. Also the build time, dependent on the chosen layer thickness and part packing density, will be analyzed. In addition, the influence of cracks has to be determined. Once the temperature effects in part-less experiments are well known, also build jobs with parts will be performed. On the one hand, the influence of built parts on the powder temperature history will help to understand and interpret the cooling process. On the other hand, the influence of different temperature histories can be directly related to specific part properties, for example the mechanical properties, the dimensional accuracy or the crystallinity. In addition the results of the temperature measurement will be transferred into a finite element simulation of the cooling process.

Acknowledgement

The authors want to thank all industry partners of the DMRC as well as the federal state of North Rhine-Westphalia and the University of Paderborn for the financial and operational support within the project “AMP²: Advanced Additive Material and Part Properties – Reduced Refresh Rates & Cooling Process Regarding LS”. Special thanks for the continuous assistance and contribution of EOS GmbH and Evonik Industries.

References

- [RDK+11] D. Rietzel, M. Drexler, F. Kühnlein, D. Drummer: Influence of temperature fields on the processing of polymer powders by means of laser and mask sintering technology, Proceedings of the Twenty-Second Annual International Solid Freeform Fabrication (SFF) Symposium, Austin (TX), USA, 2011
- [RJS14] S. Rösenberg, S. Josupeit, H.-J. Schmid: A Method to Characterize the Quality of a Polymer Laser Sinter Process, Advances in Additive Manufacturing Processes and Materials, Volume 2014, Hindawi Publishing Co., New York (NY), USA, 2014
- [RWF+12] S. Rösenberg, R. Weiffen, F. Knoop, H.-J. Schmid: Controlling the Quality of Laser Sintered Parts Along the Process Chain, Proceedings of the Twenty-Third Annual International Solid Freeform Fabrication (SFF) Symposium, Austin (TX), USA, 2012
- [SES13] S. P. Soe, D. R. Evers, R. Setchi: Assessment of non-uniform shrinkage in the laser sintering of polymer materials, The International Journal of Advanced Manufacturing Technology (2013) 68:111–125, Springer-Verlag, London, United Kingdom, 2013
- [SSG+00] J. Shen, J. Steinberger, J. Göpfert, R. Gerner, F. Daiber, K. Manetsberger, S. Ferstl: Inhomogeneous Shrinkage of Polymer Materials in Selective Laser Sintering, Proceedings of the Eleventh Annual International Solid Freeform Fabrication (SFF) Symposium, Austin (TX), USA, 2000
- [Ste01] J. Steinberger: Optimierung des Selektiven-Laser-Sinterns zur Herstellung von Feingußteilen für die Luftfahrtindustrie, Dissertation an der Technischen Universität München, Fortschrittsberichte VDI/2, 573, Düsseldorf, Germany, 2001
- [WW13] A. Wegner, G. Witt: Ursachen für eine mangelnde Reproduzierbarkeit beim Laser-Sintern von Kunststoffbauteilen, RTejournal - Forum für Rapid Technologie, Vol. 2013, Iss. 1, Cologne, Germany, 2013
- [WW14] A. Wegner, G. Witt: Understanding the Decisive Thermal Processes in Laser Sintering of Polyamide 12, Proceedings of the 30th International Conference of the Polymer Processing Society (PPS-30), Cleveland (OH), USA, 2014